Performance enhancement of pitching WECs via oscillating water columns technology

Fontana M., Sirigu S.A. and Basile D.

Abstract—**This paper describes the coupling of an oscillating U-shaped water tank, a U-tank, with a pitching floating Wave Energy Converter (WEC) to expand the response bandwidth. The performance of these energy converters strongly depends on their frequency response, and their resonance period is generally fixed once the geometric and inertial parameters of the system have been defined. The integration and appropriate control of dynamic inertial systems based on water ballast tanks enable slow tuning of the system's resonance with the incoming wave, maximizing energy extraction. The dynamic coupling of the hull with the water tank is then analyzed, and a passive control system is developed that acts on the air contained in the reservoirs of the U-tank by partitioning the volume within. Air expansion is then controlled by discretely adjusting the available, properly partitioned volume allowing the variation of the frequency response of the sloshing water tank and device. The resolution of the dynamics involves linear models based on the Boundary-ElementMethod as far as hull hydrodynamics are concerned; a solution of the Euler equation describes the oscillating tank. Finally, the expansion and compression of the air contained in the reservoirs of the U-tank are assumed to be governed by a generic polytropic transformation law, and such a condition is linearized around the operating condition. A large oscillating floating inertia-based body device is adopted as a case study, and its energy harvesting working principle is based on the gyroscope technology. The results aim to confirm the ability to perform slow tuning of the device frequency response via regulation of the air volume of the sloshing water tanks.**

Index Terms—**Passive control, Resonance, Sloshing tanks, Slow Tuning, Wave energy**

I. Introduction

THE growing demand for clean and sustainable energy sources has increased interest in harnessing energy from ocean and sea waves. By leveraging wave power, we can significantly r educe r eliance o n fossil fuels and their associated CO2 emissions, mitigating traditional energy generation's environmental impacts. Moreover, wave energy exhibits great potential and, according to the most significant c onservative estimates, assumes that the wave component accounts for around 2 TW of global power demand [1], equal to approximately 18,000 TWh annually or about 80% of our yearly electrical needs. Also, an almost enclosed sea like the Mediterranean Sea has good potential in harnessing wave energy [2]. In this context, increasing innovations on wave energy conversion systems find fertile ground, and ongoing research holds promise for improving energy extraction efficiency and expanding the overall potential of wave energy as a viable renewable resource. Given the circumstances and explanations, wave energy converter (WEC) research and technologies are relatively new in the industrial scope, since there lacks a perfectly defined technological convergence. Therefore, there are different types of wec that exploit marine phenomena in different ways.

Considering the many technologies available, the Point-Absorber [3] devices can extract energy through the relative motion between a fixed body and a floating buoy. The point-absorber technologies are compact and versatile; con, the main issue lies in the small dimensions compared to the incoming wave. An example of oscillating body, and specifically, a heaving-point-absorber (HPA) WEC is the WaveStar [4], [5], [6]. The Oscillating Water Columns (OWCs) harness energy from the oscillation of the seawater inside a chamber, converting the induced airflow into electrical energy through turbines [7], [8]. Other technical solutions are based on attenuating the wave motion responding to the wave curvature as the Pelamis device [9]. The last mentioned WEC technologies are based on the inertial phenomena of large floating bodies. Some examples are represented by the Inertial Sea Wave Energy Converter (ISWEC) [10], [11], [12] and the Pendulum Wave Energy Converter (PeWEC) [13], [14], both composed of a sealed hull and developed by the Politecnico di Torino and differentiated by the PTO system which is a gyroscope in the first mentioned case and a pendulum in the PeWEC device.

The wave energy converter system considered in this work is an oscillating WEC based on inertial properties and designed to harness the energy from ocean waves converting it into electricity through a power take-off system based on a gyroscope through the angular momentum conservation.

The principal physical phenomenon underlying WECs, especially those inertia-based, is the resonance of the conversion system with the incoming wave. While resonance can enhance energy conversion efficiency by facilitating effective energy transfer, improper resonance matching can lead to suboptimal performance and potential structural damage. When the natural frequency of a WEC's components coincides with the frequency of incident waves, resonance occurs, resulting in efficient energy absorption and amplified motion. This favourable "resonant response" maximizes power capture. However, off-resonance or anti-resonance conditions arise when the WEC's natural frequency fails to align with the incoming wave frequency. In such cases, the energy transfer becomes

M.F. and S.A.S are with the MOREnergy Lab. of the Department of Mechanical and Aerospace Engineering of Politecnico di Torino, Italy (marco fontana@polito.it). D. Basile is with the Natural Resources, Wind and Marine Energy Research Center of Eni R&D.

Digital Object Identifier: https://doi.org/10.36688/ewtec-2023-350

inefficient, causing diminished power conversion.

This work aims to enhance the resonant matching between the WEC and the incoming wave introducing a U-shaped sloshing tank to tune the floater's response. The so-called U-tank can adjust the device, shifting its resonance condition and thus harnessing energy from longer period waves. The modelling follows a performance evaluation approach regarding the RAO and response spectra of the system stressed by Jonswap spectra derived from actual wave (scatter) diagrams. The U-tank device is controlled in a slow-tuning manner modifying its resonance period acting on discrete volumes in which the air within can be expanded and compressed, thus modulating its stiffness.

The paper is structured as follows: Section II presents the mathematical formulation encompassing the wave spectra, the ISWEC test case, and the U-tank system. Subsequently, the chapter delves into the coupling of the devices by parameterizing the U-tank system while considering the feasibility constraint of the hull. Section IV expounds on the passive control strategy for slow-tuning employed by the U-tank. Finally, the simulations conducted in regular (sec.V-A) and irregular (sec.V-B) waves are detailed, and the corresponding outcomes are presented.

II. Mathematical modelling - Wave and Devices

In this section, the wave formulation is described in terms of Jonswap Spectrum, the both the WEC and the U-tank are described and their mathematical models are presented.

A. Wave Spectra

The ocean and sea waves have several components that depend on time and location. A heuristic and general description of the waves can be conducted with a statistical approach defining the energy density distribution over the wave period. In this work, the directionality of the waves is neglected in that the floating device bases its principle of operation on pitching motion and thus can be oriented through its mooring system to receive the wave by realizing a definite direction with it. This assumption also requires considering a highly directional marine site. The WEC device of this work is conceived to be installed in the Strait of Sicily in the Mediterranean Sea, a fetch-limited sea in which a more proper spectrum modelling is the JONSWAP spectrum, with respect to the Table A.4 of [15]. The JONSWAP model was derived considering that the more commonly used Pierson-Moskowitz spectrum does not fit properly a non-fully developed sea, so the latter can be enhanced by multiplying it with an extra peak enhancement factor γ:

$$S(\omega) = A_g \frac{(H_{m0}/4)^2}{\omega_p} \gamma G_0 \omega_n^{-N} \exp\left(\frac{-N}{M\omega_n^M}\right) \quad (1)$$

Where A_g represents a normalization faction used when $\gamma > 1$, H_{m0}, or H_s is the significant wave height, the angular peak frequency ω_p, G_0 is a normalizing factor related to Bretschneider form (JONSWAP with $\gamma = 1$), ω_n is the array of angular frequencies normalized over the peak frequency, finally the parameters M and N define the spectral width around the peak and the decay of high frequency side respectively. The plot in Fig.1 enlights the comparison between JONSWAP and Pierson-Moskowitz spectra for the same values of significant wave height H_s and energetic period T_E. the formulation used in this work refers to [15] in which the peak period and the energetic period depend on the peak enhancement factor as follows:

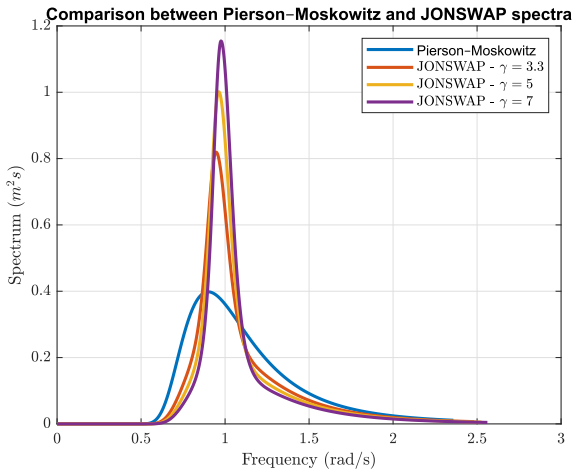

Fig. 1. The Pierson-Moskowitz and JONSWAP spectra comparison considering a significant wave height $H_s = 2m$ and energetic period $T_E = 6s$. The peakness of the JONSWAP spectrum is the higher the greater the value of γ which is unit in the case of Pierson–Moskowitz.

$$T_p = \frac{T_E}{0.8255 + 0.03852\gamma - 0.005537\gamma + 0.0003154\gamma} \quad (2)$$

B. Floating WEC

The Wave Energy converter considered in the scope of this work is the Inertia Sea Wave Energy Converter [10]. The floater has a cradle-shaped hull parametrically identified by circles, as shown in Fig.1 of [12] and is optimized for a given marine site [16].By capitalizing on the inertial coupling between the floater and the gyroscopic unit inside, the device effectively eliminates the requirement for any moving parts to come into contact with the seawater. The following Fig.2 from [17] enlights the cradle-shaped hull, the gyroscope sealed within, the PTO unit and the incoming wave direction. Upon a more detailed examination of the gyroscopic conversion principle for pitch motions, we can observe that the device's main coordinate system aligns its x-axis towards the bow, representing the wave direction. Simultaneously, the y-axis corresponds to the pitching motion induced by the waves, denoted as δ. By combining the rotational speed of the flywheel ($\dot{\phi}$) with the hull's pitching velocity ($\dot{\delta}$), a gyroscopic torque is generated around the ε-axis. This torque is utilized to drive an electrical generator, allowing the extraction of energy from incoming waves. The dynamics of the gyroscope can be derived from Euler's equation, where equilibrium is imposed at the Power Take-Off (PTO) shaft [18]. The PTO torque is governed by a control law

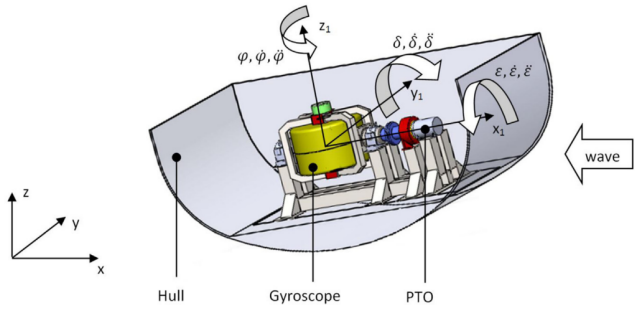

Fig. 2. WEC layout with the gyroscopic unit sealed in the hull, and its flywheel spins around the ϕ-axis. The PTO is in-line with the precession axis ε. The floater oscillates around the pitch-axis δ.

(Eq. 3), which consists of a first component in phase with velocity (active term) and a second reactive term in quadrature with the rate:

$$T_{PTO} = k\varepsilon + c\dot{\varepsilon} \tag{3}$$

The Cummins Equation describes the hydrodynamic model [19] using the six degrees of freedom time-domain equation for a rigid floating body:

$$(\mathbf{M} + \mathbf{A}_\infty)\,\ddot{X} + \int_0^t \mathbf{h_r}(t-t')\dot{X}dt' + \mathbf{K}X = F_w + F_g \tag{4}$$

In the given expression, the first term corresponds the mass matrix $\mathbf{M}$, the second term represents the constant positive definite added mass for infinite frequency $\mathbf{A}_\infty$. the damping term in the convolution integral incorporates the impulse response functions $\mathbf{h_r}$ of the radiation forces. The stiffness term $\mathbf{K}$ refers to the hydrostatic stiffness matrix. On the right-hand side (RHS), we have the wave forcing (F_w) and the gyroscope's reaction forces (F_g). To facilitate the analysis, it is advantageous to transform the equation into the frequency domain using the following approach:

$$(\mathbf{M} + \mathbf{A}(\omega))\,\ddot{X}(\omega) + \mathbf{B}(\omega)\dot{X} + \mathbf{K}X(\omega) = F_w(\omega) + F_g(\omega) \tag{5}$$

Except for the gyroscopic reaction, the terms described above can be obtained through numerical tools based on the Boundary Element Method (BEM), such as NEMOH [20], [21]. Once the floater is defined, its behaviour under operating waves and conditions is determined by the Response Amplitude Operator (RAO), which are effectively transfer function of the response amplitude of the floater with respect to the amplitude of the incoming wave.

C. U-tank

The oscillating U-shaped sloshing tank, also called U-tank, the concept was initially developed by Frahm [22], and Froude [23] intending to obtain an Anti-Resontant-Tank (ART) to mitigate the roll motion in the naval application. In recent years, the application of U-tank devices has expanded to include the civil engineering field, specifically as anti-resonant devices for skyscrapers. The U-tank devices, when used in the context of skyscrapers, serve as tuned mass dampers (TMDs) or vibration control systems. By strategically incorporating U-tank devices into the structural design of tall buildings, the aim is to reduce the resonant response and enhance the building's overall performance under dynamic loading, such as wind-induced vibrations or seismic events. In the scope of wave energy the U-shaped sloshing tanks are mainly used coupled with Wells turbine-based systems to extract energy from pressure differences induced by the movement of water columns [7], [24].

The mathematical model of the U-tank was derived by Lloyd [25] from the Euler's equation coupling the continuity and momentum conservation equations, leading to the following monodimensional law:

$$\frac{\partial v}{\partial t} + v\frac{\partial v}{\partial y} = Y - \frac{1}{\rho}\nabla p \tag{6}$$

where v is the fluid velocity along the curvilinear direction y, as shown in Fig.3. The first term at RHS contains the external forces per unit mass induced by the gravity, the acceleration of the external motion, the frictional and damping forces. Finally, the density of the fluid within is ρ and the pressure field is p. The

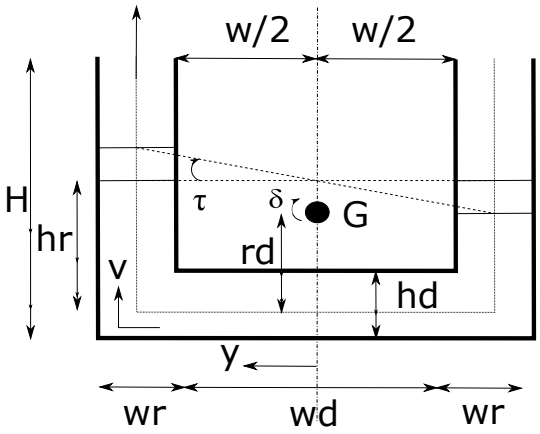

Fig. 3. Utank scheme and geometrical definitions with respect to the hull centre of gravity G and imposed pitch motion δ

Eq.6 carries with it the following assumptions: one-dimensional fluid (water) motion, external motion only in pitch-direction δ, velocity gradient along the perpendicular axis to the y-axis can be neglected as well as the corner effects at the elbows. The last one is a strong assumption as enlighted in [26] where the comparison between a sharp-corner and rounded devices is made through Computational Fluid Dynamics simulations.

The geometrical properties in Fig.3 refers to the the total height H, the fluid level at rest from the centerline of the horizontal duct h_r, the height of the latter is h_d and its width is w_d. The vertical tanks, henceforth called reservoirs, are defined by the width w_r. Regarding the coupling with the floater the distance between the centerline of the horizontal duct and the WEC's center of gravity is defined by r_d. Finally, the water angle τ is defined as the angle between the water level and the one at the equilibrium position.

III. U-TANK AND FLOATER COUPLING

The water angle τ and the coupling with WEC in pitch motion δ lead to the expression of Eq.6 in a

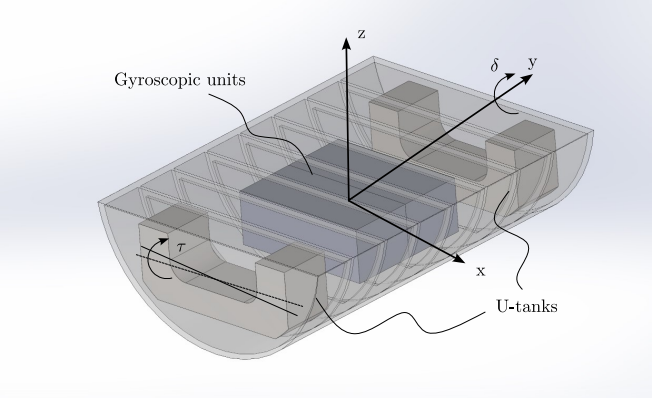

Fig. 4. Example of pairing between WEC hull and gyroscopes, and two U-tank devices

canonical non-dimensional form [27]:

$$a_{\tau\tau}\ddot{\tau} + b_{\tau\tau}\dot{\tau} + c_{\tau\tau}\tau = -\left[a_{\tau 5}\ddot{\delta} + c_{\tau 5}\delta\right] \tag{7}$$

The Eq.7 represents a 1 DOF lumped parameter model in which the U-tank, described by a mass-damper-spring system is coupled in pitch-motion with the floater. The subscript '5' refers to the pitch motion as the fifth term of the X term in the Eq.4. The coefficient in the lumped-parameter model are defined as follows:

- $a_{\tau\tau} = Q_t w_r \left(\frac{w}{2h_d} + \frac{h_r}{w_r}\right)$
- $b_{\tau\tau} = Q_t q w_r \left(\frac{w}{2h_d^2} + \frac{h_r}{w_r^2}\right)$
- $c_{\tau\tau} = Q_t g$
- $a_{\tau 5} = Q_t\,(r_d + h_r)$
- $c_{\tau 5} = c_{\tau\tau}$
- $Q_t = \frac{1}{2}\rho w_r w^2 x_t$

Where the variable w is the distance between the vertical centerlines of the reservoirs ($w = w_r + w_d$), and q incorporates viscous damping effects identifiable from free-decay tests conducted through experiments or simulations using CFD models. The Fig.4 schematizes the U-tank and WEC hull pairing considering two gyroscope units (bounded boxes) and two U-tank devices in aft and fore sides. The WEC system is given for a specific marine site after a techno-economic optizimization [14], defining its dimensions, the inertial properties regarding both the hull and the gyroscopic units.

The introduction of the U-tank device (the two units can be modelled as a singular device with an equivalent extrusion $x_{teq} = 2x_t$ in pitch-direction), achieves an expansion of the degrees of freedom of the system leading to a 8-DOF system:

$$\begin{aligned} X = [&x : \text{Surge}, y : \text{Sway}, z : \text{Heave},\\ &\chi : \text{Roll}, \delta : \text{Pitch}, \psi : \text{Yaw},\\ &\varepsilon : \text{Gyroscope}, \tau : \text{Utank}]^T \end{aligned}$$

The pairing of the U-tank device within the floater is performed considering the geometrical and inertial feasibilty. The input properties to generate a feasibile coupling are:

- MR: Mass ratio of the U-tank over the floater mass. This parameter defines the U-tank mass and affects the ballasts in the hull's aft and fore sides, adjusting them to accommodate the insertion of the U-tank and its mass.
- h_r/H: Water level ratio over the available total height%.
- w_d/W: Horizontal duct width over the total available width.
- T_{res}: Uncoupled frequency of the U-tank. This parameter represets the natural frequency of the U-tank device, leading to the computation of the horizontal duct height.
- x_{hull}: position of the low-left corner point of the U-tank as shown in Fig defined from 0 to 1 starting from the lowest point in z-axis of the hull profile at the same point of the gyro unit unitl hull-profile locate at the left-side ballast XoZ-plane. This one parameter allows to define the maximum available height and width of the U-tank.

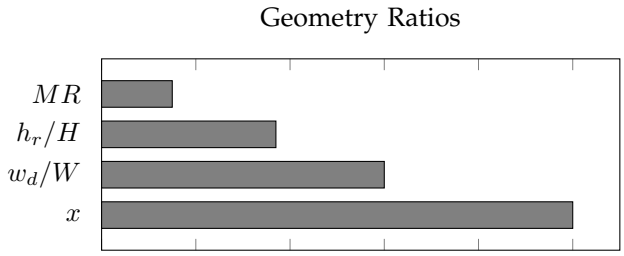

Fig. 5. Geometry ratios as input of this case study

The above mentioned geometry ratios and imposing an uncoupled resonance period of the U-tank $T_{res} = 12s$ define the feasible U-tank shown in Fig.6. The Mass

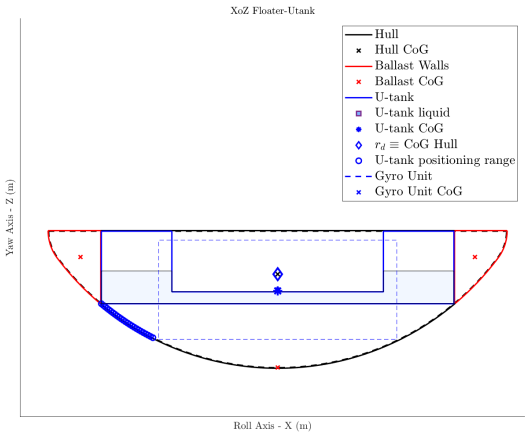

Fig. 6. Geometrical coupling of the floating WEC hull and gyroscopes, and two U-tank devices in the XoZ plane (lateral view)

Ratio MR lead also to the U-tank length (y-axis) as shown in the plan view of Fig.7 increasing the sizing along the pitch axis in accordance with the location and the dimensions of the gyroscopic units that represent a feasibility constraint.

The coupling between the WEC test case (resonance at $6s$) and the U-tank system (resonance at $12s$) generates a typical 4^{th}order system as shown in Fig.8. Note

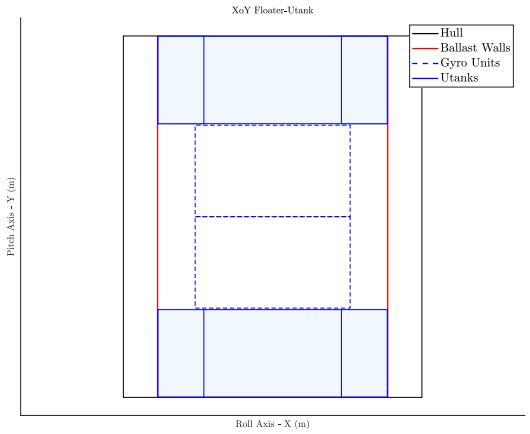

Fig. 7. Geometrical coupling of WEC hull and gyroscopes, and two U-tank devices in the XoY plane (plan view)

that the anti-resonance condition occurs at the peak in the RAO of the U-tank system.

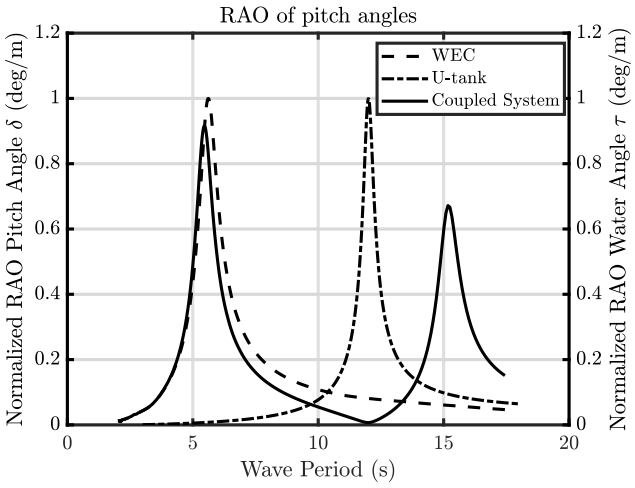

Fig. 8. Resulting Response Amplitude Operator of pitch angle (δ) and water angle (τ) from coupling the WEC test case with the U-tank device

IV. U-TANK PASSIVE CONTROL STRATEGY

In this section, the U-tank slow-tuning technique is described and modelled. The concept involves enhancing the performance of Wave Energy Converters (WECs) by introducing an adjustable U-tank system. This approach aims to enable WECs to operate effectively even under wave conditions for which they were not originally designed at a certain operating wave period at which resonance occurs. The choise was made to adjust the U-tank stiffness acting on the air contained within sealing the device in the WEC's hull making two basic points about not using elements that require power and not acting on the water contained in the sloshing tanks because of its density ratio with respect to the air phase and the related and resulting inertial loads. Consider the following scheme in Fig.9 of an equivalent U-tank device (due to the assumption in the LLoyd model) with the length (normal direction) $x_{t_{eq}} = n_{Utank} x_t$, where n_{Utank} is the number of U-tank devices, each of the air columns in the Aft ('A') and Fore ('F') sides occupies a volume that depends on the initial one and on the water level (angle τ):

$$V_{F,A} = V_0 \mp b\tau \tag{8}$$

where $b = \frac{w}{2} x_{t_{eq}} w_r$ is the moment arm times the freesurface area with the assumption of small angles and the consequent approximation of the water level $z = \frac{w}{2}\tan(\tau) \approx \frac{w}{2}\tau$.

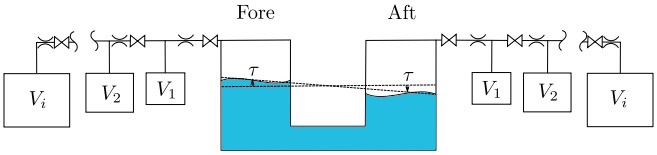

Fig. 9. U-tank scheme with the expansion volume in the general case of both reservoirs connected

Let us consider that the reservoirs are connected to i added volumes in series expansion. The resulting added volume has an equivalent size of V_e, allow the air within the reservoirs to expand or compress. This transformation follows a generic polytropic law with an exponent of n. The polytropic law is expressed between a generic time τ (which is a function of time t) and the initial state:

$$pV^n = p_0 \left(V_0 + V_e\right)^n = p_0 a^n \tag{9}$$

Once the reservoir is connected to the added i-volumes, its volume becomes, from Eq.8:

$$V_{F,A} = V_0 + V_e \mp b\tau = a \mp b\tau \tag{10}$$

This architecture realizes a pressure difference between the fore and aft sides which can be linearized around the equilibrium condition $\tau \approx 0$:

$$\Delta p = p_0 a^n \left(\frac{1}{(a - b\tau)^n} - \frac{1}{(a + b\tau)^n}\right) \approx \frac{2p_0 bn}{a}\tau + \mathcal{O}(\tau^2) \tag{11}$$

The linearized pressure difference acts on the free-surfaces of water generating a torque which depends on the water angle, so acts like a stiffness in Eq.7:

$$T_{air} = \frac{x_{t_{eq}} w_r w}{2}\Delta p \approx \frac{2p_0 b^2 n}{a}\tau = c_{air}\tau \tag{12}$$

The dynamic equation that coupled the U-tank and the floater becomes:

$$a_{\tau\tau}\ddot{\tau} + b_{\tau\tau}\dot{\tau} + \left(c_{\tau\tau} + c_{air}\right)\tau = -\left[a_{\tau 5}\ddot{\delta} + c_{\tau 5}\delta\right] \tag{13}$$

The inclusion of additional volumes introduces an incremental stiffness component ($c^*_{\tau\tau} = c_{\tau\tau} + c_{air}$) to the system, enabling discrete tuning of the resonance condition. This tuning is achieved by manipulating the valves within the series connections. To be noted that different layouts, i.e. only one of the reservoirs connected to the added volume and the reaming to the atmosphere, generate an added stiffness which is half of that previously derived. The identification of the maximum available volume can be perfomed in the generation the feasible U-tank as previously described and both the layout generate the increasing of the

stiffness according to the ratio that depends on the added volumes as shown in Fig.:

$$\frac{c_{\tau\tau} + c_{air}}{c_{\tau\tau}} = \frac{c^*_{\tau\tau}}{c_{\tau\tau}} \tag{14}$$

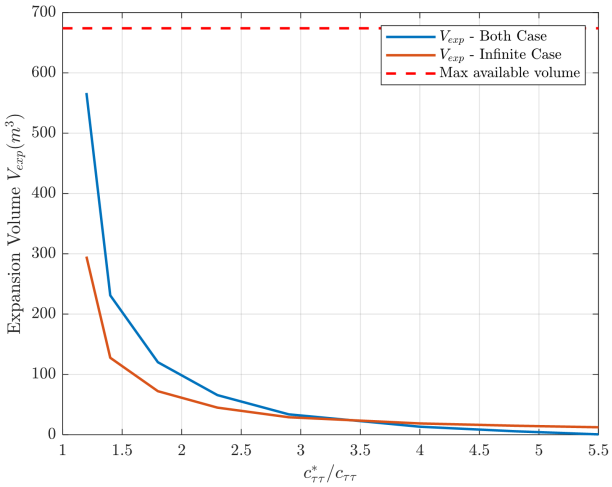

Fig. 10. Dependency of added stiffness ratio on added volumes considering the maximum available volume for the specific WEC test case. The *"Both"* case indicate that both the reservoirs are connected to the added volume, viceversa the *"Infinite"* case refers to one reservoir open to atmosphere.

V. Results

This results section is organized as follows: the flowchart in Fig.11 describes the steps of the simulations starting with a known float consisting of hull, ballast, and gyro units, whose RAO is then defined. This is coupled with a feasible utank identified by the parameters described earlier by keeping the WEC weighing constant. We then define the layout of the expansion volumes and the desired resonance period through the additional stiffness being the angular frequency of resonance equal to:

$$\omega_{res} = \sqrt{\frac{c_{\tau\tau} + c_{air}}{a_{\tau\tau}}} \Rightarrow T_{res} = \frac{2\pi}{\omega_{res}} \tag{15}$$

at this point the previously described 8Dof system matrices are defined with the U-tank modified through the expansion volumes, and the pitching RAO is calculated. For each modified U-tank a frequency domain analysis is conducted to computed the response spectra for different wave spectra. All the results are computed in the gyroscope off condition.

A. Regular wave analysis - Response Amplitude Operator

As anticipated in the section III, the first performance indicator of the WEC device working in pitch is the transfer function of motion, or *Response Amplitude Operator* (RAO) of the complete 8DOF system is computed as follow:

$$\mathbf{RAO} = \frac{F_e(\omega)}{-\omega^2(\mathbf{M} + \mathbf{A}(\omega)) + \imath\omega\mathbf{B}(\omega) + \mathbf{K}} \tag{16}$$

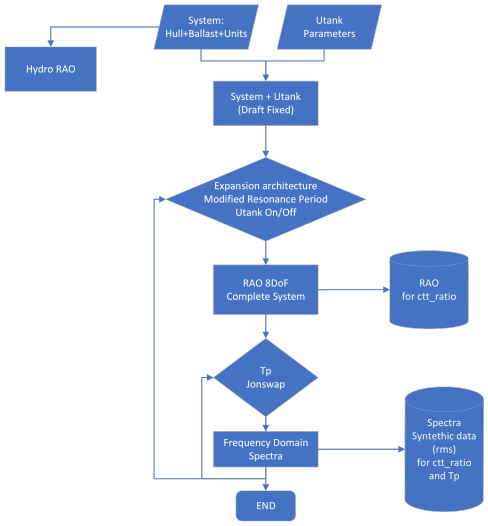

Fig. 11. Simulation steps and results flow-chart

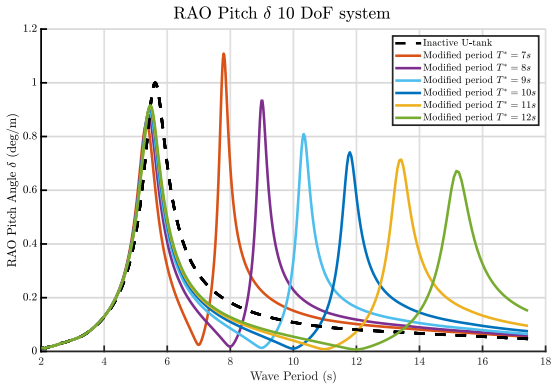

Fig. 12. RAO of pitch angle δ as modified period changes

TABLE I
Cases of regular wave simulation

Modified period	Stiffness ratio	Added volume
$T^*(s)$	$\frac{c^*_{\tau\tau}}{c_{\tau\tau}}$ ()	$V_e\ (m^3)$
7	2.9	3.6
8	2.3	20.2
9	1.8	48.7
10	1.4	106.6
11	1.2	281.8
12	1	∞

Since the operating principle of WEC depends on the pitching motion, the results refer to the angle δ, as the added stiffness ratio changes.

The results in Fig.12 show a modification of the pitch angle RAO increasing the stiffness of the system, from the right-side green line (orginal U-tank period of $12s$) to the red line corresponding to a modified period of $7s$. The Table I resumes the relation between the modified periods T^* in Fig.12, the relative stiffness ratio $c^*_{\tau\tau}$ and the corresponding added volume.

B. Irregular wave anlysis - Spectra

The irregular wave anlysis involves the wave spectra definition. For the specific test case the Pantelleria scatter matrix, shown in Fig.13 is considered [2] and three spectra are extrapolated from the isosteepness wave, i.e. keeping constant the ratio of the wave height over the wavelenght equal to $1/30$. The system response $\mathcal{S}(\omega)$ in irregular waves with spectrum $\mathcal{S}_w(\omega)$ is computed from the previously derived **RAO** as follows:

$$\mathcal{S}(\omega) = |\mathbf{RAO}|^{\mathbf{T}} \mathcal{S}_w(\omega) \mathbf{RAO} \tag{17}$$

The combination of significant wave height H_s, energetic period T_e, and the JONSWAP peakness γ is resumed in Table II. The additional three spectra cases, in combination with the previous six modified U-tanks, lead to 18 spectra, thus, for clarity sake, only the extreme cases are reported in Figs.14 and 15.

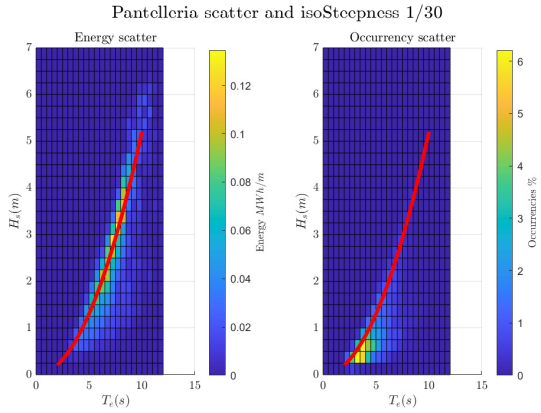

Fig. 13. Pantelleria scatter matrix

TABLE II
CASES OF IRREGULAR WAVE SIMULATION

Significant Wave Height	Energetic Period	Peakness
$H_s(m)$	$T_e(s)$	γ
1.4	5.0	3.3
2.6	7.0	3.3
4.0	8.5	3.3

A more informative outcome for comparison with the 7-degree-of-freedom (DOF) system is the calculation of the root mean square (RMS) value of the pitch angle . By considering the equation for the fifth DOF (δ) and analyzing the spectra depicted in the Figs.14,15, we can extract the RMS value using its definition:

$$\delta_{RMS} = \int_{\omega} \mathcal{S}(\omega)\omega \tag{18}$$

which is compared to the WEC-only system as reported in the following results of Fig.16. The findings indicate a notable increase in hull pitching and potentially improved hull productivity when the U-tank device is exposed to irregular waves with extended peak periods. This increase is directly proportional to the energy period and significant wave height. However, as we approach the design conditions of the 7-DOF system, for which the U-tank device is specifically designed, the performance starts to decline.

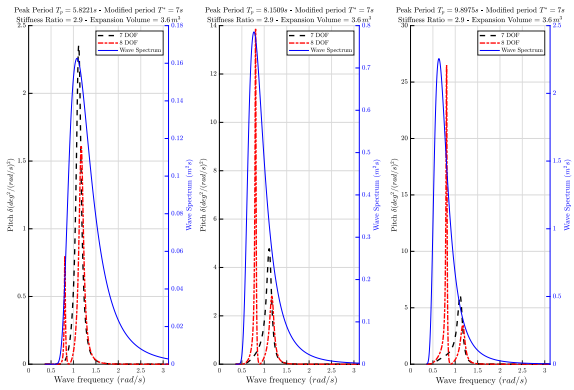

Fig. 14. Spectra for maximum stiffned U-tank case ($T^* = 7s$). From the left to right increasing value of H_s-T_e. Dashed black line - - - - refers to the WEC only (7 DOF), dotted red line ·-·-·-· refers to the coupled system (8 DOF), continuous blue line ——— refers to the wave spectrum.

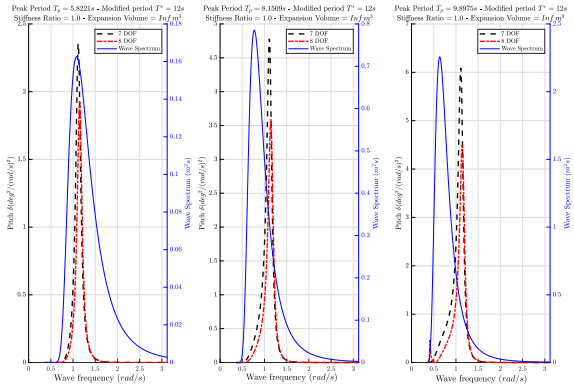

Fig. 15. Spectra for the unmodified U-tank case ($T^* = 12s$). From the left to right increasing value of H_s-T_e. Dashed black line - - - - refers to the WEC only (7 DOF), dotted red line ·-·-·-· refers to the coupled system (8 DOF), continuous blue line ——— refers to the wave spectrum.

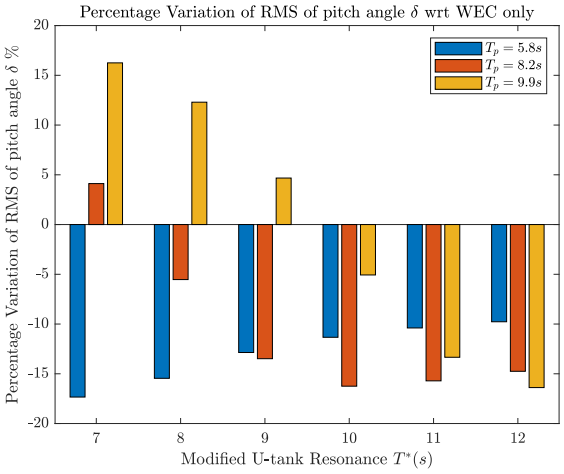

Fig. 16. The comparison involves the pitch angle of the systems in the irregular wave analysis as percentage variation with respect to the 7DOF case. The outcomes are sorted based on increasing wave peak period T_p and decreasing stiffness of the U-tank

VI. Conclusion

This work emphasizes the capabilities of the U-shaped sloshing tank system, tuned by a novel system of discrete volumes, to enhance the performance of a pitch-based wave energy converter both in regular and irregular wave through frequency domain analysis. The device exhibits enhanced capabilities when operating in conjunction with long waves. Defining the performance of the pitching-WEC as proportional to the amplitude of its oscillation in pitch motion, it can be state that the histogram in Fig.16 points out that as the U-tank device becomes stiffener, shortening its resonance condition thought lower values of the discrete additional volumes, there is an enhancement in the range of about 8 to $10\,s$ which are long waves compared to the operative waves of the WEC-only device.

However, it is worth noting that the WEC device is primarily designed for seas characterized by relatively short waves. The results indicate potential for improvement by incorporating the device into the optimization process upstream of the flow-chart in Fig.11 This would involve shifting the operating conditions to align with those specific to ocean seas, thus maximizing its performance and effectiveness.

Future works will exploit this novel architecture to control the stiffness of the U-tank through experiments in which the presented model will be validated through a Hardware-in-the-Loop architecture implemented in a Stewart platform considering the complete motion and the coupling between the WEC and controlled U-tank.

References

[1] K. Gunn and C. Stock-Williams, "Quantifying the global wave power resource," *Renewable Energy*, vol. 44, pp. 296–304, aug 2012.

[2] G. Mattiazzo, "State of the Art and Perspectives of Wave Energy in the Mediterranean Sea: Backstage of ISWEC," *Frontiers in Energy Research*, vol. 7, p. 114, oct 2019. [Online]. Available: https://www.frontiersin.org/article/10.3389/fenrg.2019.00114/full

[3] M. Rava, P. Dafnakis, V. Martini, G. Giorgi, V. Orlando, G. Mattiazzo, G. Bracco, and A. Gulisano, "Low-Cost Heaving Single-Buoy Wave-Energy Point Absorber Optimization for Sardinia West Coast," *Journal of Marine Science and Engineering*, vol. 10, no. 3, 2022.

[4] M. Kramer, L. Marquis, and P. Frigaard, "Performance evaluation of the wavestar prototype," in *9th ewtec 2011: Proceedings of the 9th European Wave and Tidal Conference, Southampton, UK, 5th-9th September 2011*. University of Southampton, 2011.

[5] R. H. Hansen and M. M. Kramer, "Modelling and control of the wavestar prototype," in *Proceedings of the 9th European Wave and Tidal Energy Conference, EWTEC 2011*. University of Southampton, 2011.

[6] N. Faedo, Y. Peña-Sanchez, E. Pasta, G. Papini, F. D. Mosquera, and F. Ferri, "Swell: An open-access experimental dataset for arrays of wave energy conversion systems," *Renewable Energy*, 2023.

[7] A. F. O. Falcão and P. A. Justino, "OWC wave energy devices with air flow control," *Ocean Engineering*, vol. 26, no. 12, pp. 1275–1295, 1999.

[8] B. Fenu, M. Bonfanti, A. Bardazzi, C. Pilloton, A. Lucarelli, and G. Mattiazzo, "Experimental investigation of a multi-owc wind turbine floating platform," *Ocean Engineering*, vol. 281, p. 114619, 2023. [Online]. Available: https://www.sciencedirect.com/science/article/pii/S002980182301003X

[9] R. Henderson, "Design, simulation, and testing of a novel hydraulic power take-off system for the pelamis wave energy converter," *Renewable energy*, vol. 31, no. 2, pp. 271–283, 2006.

[10] G. Bracco, E. Giorcelli, and G. Mattiazzo, "ISWEC: A gyroscopic mechanism for wave power exploitation - ScienceDirect." [Online]. Available: https://www.sciencedirect.com/science/article/abs/pii/S0094114X11001091

[11] M. Bonfanti, A. Hillis, S. A. Sirigu, P. Dafnakis, G. Bracco, G. Mattiazzo, and A. Plummer, "Real-time wave excitation forces estimation: An application on the iswec device," *Journal of Marine Science and Engineering*, vol. 8, no. 10, 2020. [Online]. Available: https://www.mdpi.com/2077-1312/8/10/825

[12] G. Giorgi, S. Sirigu, M. Bonfanti, G. Bracco, and G. Mattiazzo, "Fast nonlinear Froude – Krylov force calculation for prismatic floating platforms : a wave energy conversion application case," *Journal of Ocean Engineering and Marine Energy*, vol. 7, no. 4, pp. 439–457, 2021. [Online]. Available: https://doi.org/10.1007/s40722-021-00212-z

[13] N. Pozzi, A. M. Bonetto, M. Bonfanti, G. Bracco, P. Dafnakis, E. Giorcelli, B. Passione, S. A. Sirigu, and G. Mattiazzo, "Pewec: Preliminary design of a full-scale plant for the mediterranean sea," 2018.

[14] S. A. Sirigu, "Techno-Economic optimisation for a wave energy converter via genetic algorithm," *Journal of Marine Science and Engineering*, vol. 8, no. 8, 2020.

[15] Y. ying Wang, "The specialist committee on waves final report and recommendations to the 23 rd ittc," 2016.

[16] S. A. Sirigu, G. Vissio, G. Bracco, E. Giorcelli, B. Passione, M. Raffero, and G. Mattiazzo, "ISWEC design tool," *International Journal of Marine Energy*, vol. 15, pp. 201–213, 2016. [Online]. Available: http://dx.doi.org/10.1016/j.ijome.2016.04.011

[17] G. Bracco, A. Cagninei, E. Giorcelli, G. Mattiazzo, D. Poggi, and M. Raffero, "Experimental validation of the ISWEC wave to PTO model," *Ocean Engineering*, vol. 120, pp. 40–51, jul 2016.

[18] G. Bracco, E. Giorcelli, G. Mattiazzo, M. Pastorelli, and M. Raffero, "Testing of a gyroscopic Wave Energy System," *2012 International Conference on Renewable Energy Research and Applications, ICRERA 2012*, no. M, 2012.

[19] W. Cummins, "The impulse response function and ship motions," Department of the navy, Tech. Rep., 1962.

[20] A. Babarit and G. Delhommeau, "Theoretical and numerical aspects of the open source BEM solver NEMOH," sep 2015. [Online]. Available: https://hal.archives-ouvertes.fr/hal-01198800

[21] *Second Order Difference- and Sum-Frequency Wave Loads in the Open-Source Potential Flow Solver NEMOH*, ser. International Conference on Offshore Mechanics and Arctic Engineering, vol. Volume 5A: Ocean Engineering, 06 2022, v05AT06A019. [Online]. Available: https://doi.org/10.1115/OMAE2022-79163

[22] H. H. Frahm, "RESULTS OF TRIALS OF THE ANTI-ROLLING TANKS AT SEA," *Journal of the American Society for Naval Engineers*, vol. 23, no. 2, pp. 571–597, mar 1911. [Online]. Available: http://doi.wiley.com/10.1111/j.1559-3584.1911.tb04595.x

[23] W. Froude, "On the rolling of Ships," Tech. Rep., 1861.

[24] N. Fonseca and J. Pessoa, "Numerical modeling of a wave energy converter based on U-shaped interior oscillating water column," *Applied Ocean Research*, vol. 40, pp. 60–73, 2013.

[25] A. Lloyd, "Seakeeping – Ship Behaviour in Rough Weather. A. R. J. M. Lloyd. 486 pages, 17 × 24.5 cm, Ellis Horwood, 1989." *Journal of Navigation*, vol. 43, no. 1, pp. 140–140, jan 1989.

[26] M. Fontana, S. A. Sirigu, and M. Bonfanti, "Study of u-shaped sloshing tanks to tune wave energy converters through high-fidelity cfd simulations as geometry changes," in *2022 International Conference on Electrical, Computer, Communications and Mechatronics Engineering (ICECCME)*, 2022, pp. 1–6.

[27] S. A. Sirigu, M. Bonfanti, P. Dafnakis, G. Bracco, G. Mattiazzo, and S. Brizzolara, "Pitch Resonance Tuning Tanks: A novel technology for more efficient wave energy harvesting," in *OCEANS 2018 MTS/IEEE Charleston, OCEAN 2018*. Institute of Electrical and Electronics Engineers Inc., jan 2019.